

Supporting Information

Incorporating gold nanoclusters and target-directed liposomes as a synergistic amplified colorimetric sensor for HER2-positive breast cancer cell detection

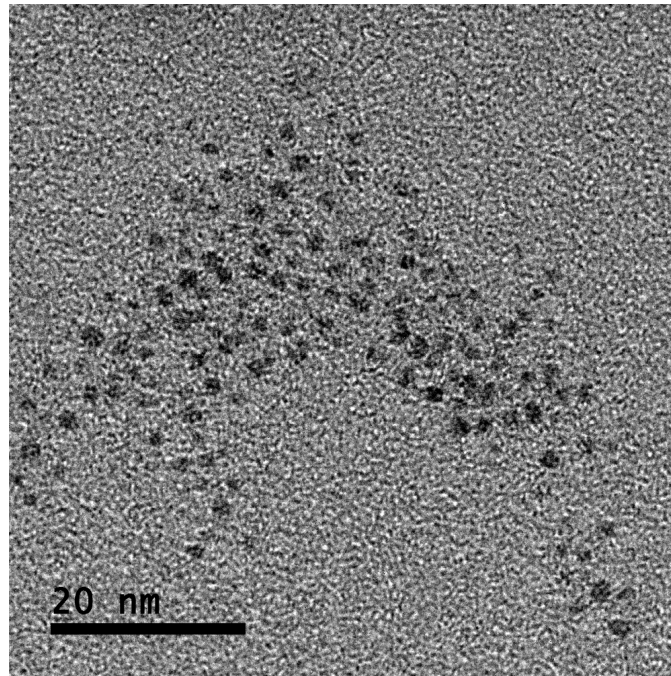


Figure S1. The TEM image of the BSA-AuNCs.

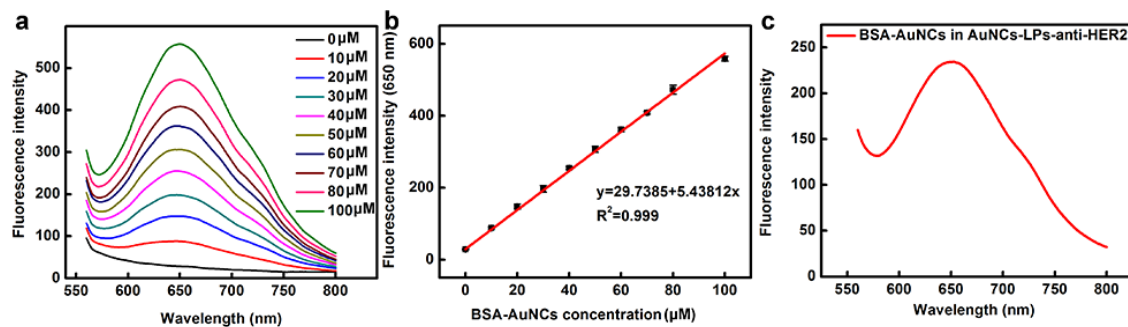


Figure S2. Testing the ratio of BSA-AuNCs and liposomes in BSA-AuNCs-LPs-anti-HER2. (a) The fluorescence spectra of BSA-AuNCs with known concentrations in PBST. The concentration of BSA was adopted to confirm the concentration of BSA-AuNCs. (b) The linear relationship between fluorescence intensity at 650 nm and the concentration of

BSA-AuNCs. (c) The fluorescence spectrum of BSA-AuNCs in AuNCs-LPs-anti-HER2 dispersed in PBST. The ratio of BSA-AuNCs : liposome is calculated to be 1925 : 1.

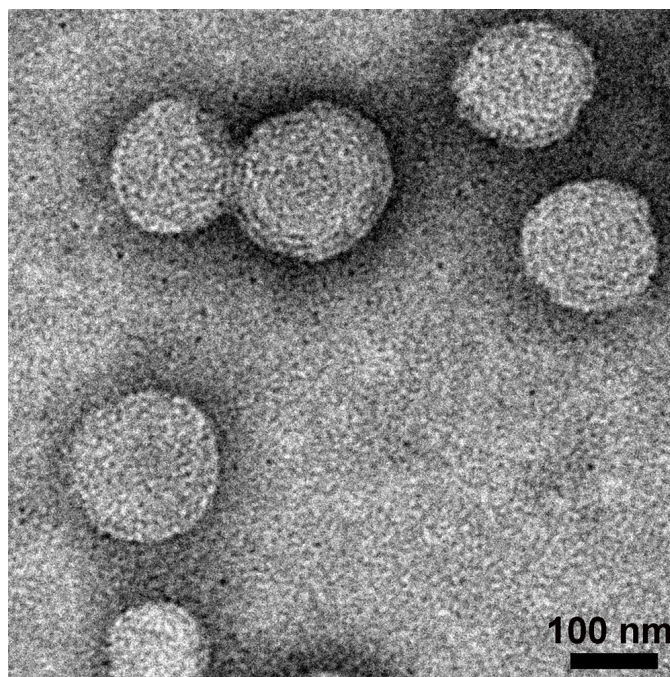


Figure S3. The TEM image of the AuNCs-LPs.

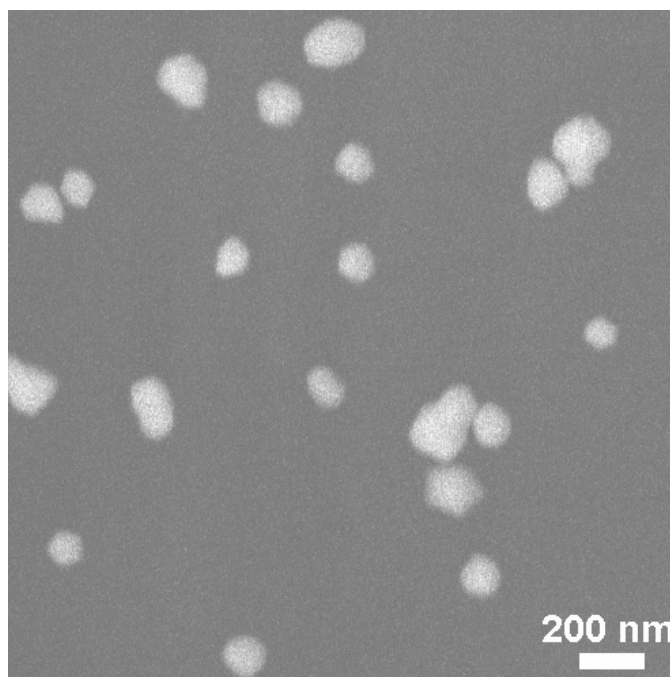


Figure S4. The SEM image of the AuNCs-LPs.

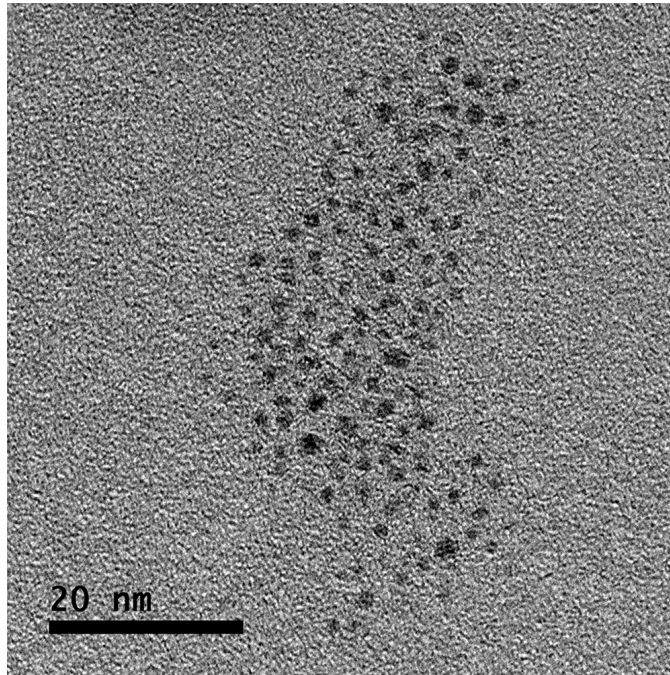


Figure S5. The TEM image of the AuNCs dispersed in PBST.

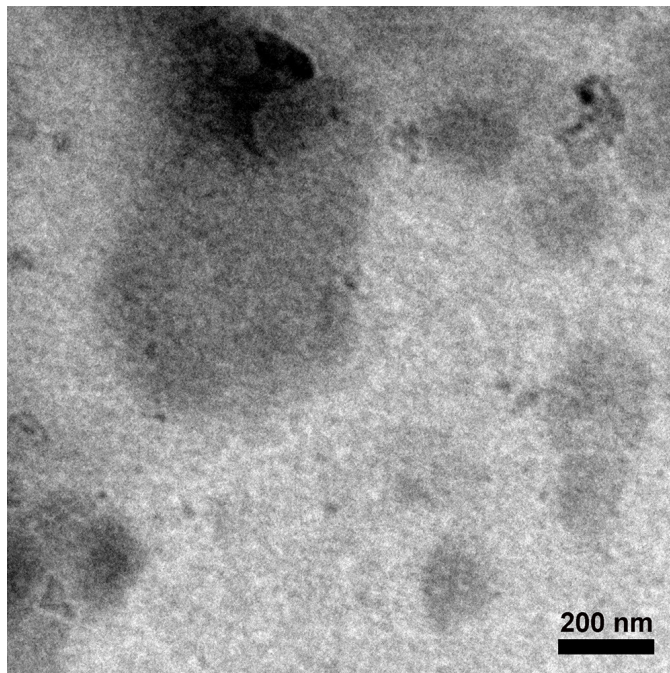


Figure S6. The TEM image of BSA-AuNCs-LPs-anti-HER2 after exposition to PBST. The image does not show any vesicular structures.

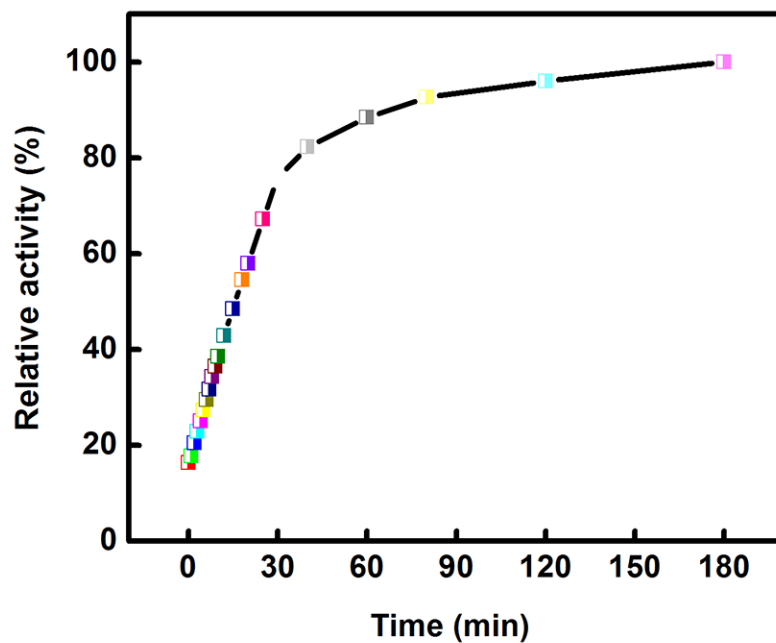


Figure S7. Catalytic activity of BSA-AuNCs-LPs-anti-HER2 as a function of incubation time.

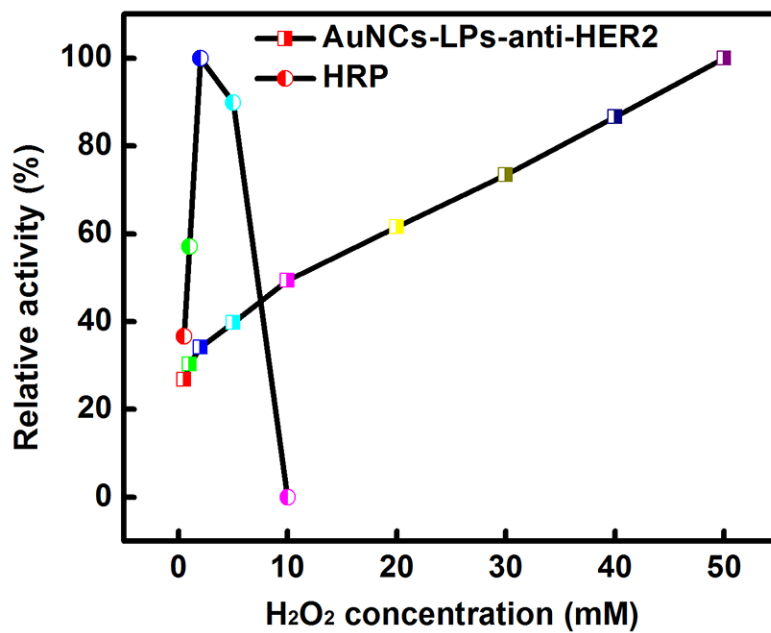


Figure S8. The peroxidase-like activity of the BSA-AuNCs-LPs-anti-HER2 is dependent on H₂O₂ concentration.

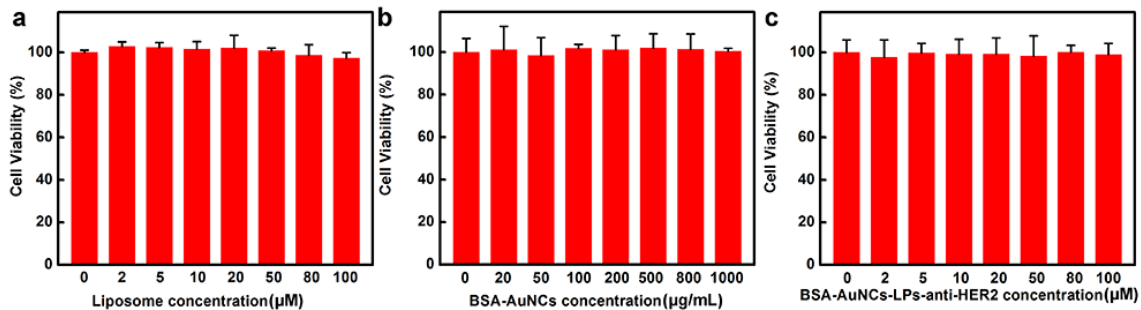


Figure S9. Cytotoxicity testing results of liposome, BSA-AuNCs and BSA-AuNCs-LPs-anti-HER2 against SKBR3 cells by MTT assays. The concentration of the liposome was adopted to confirm the concentration of BSA-AuNCs-LPs-anti-HER2. Error bars represent standard deviation of three independent measurements.

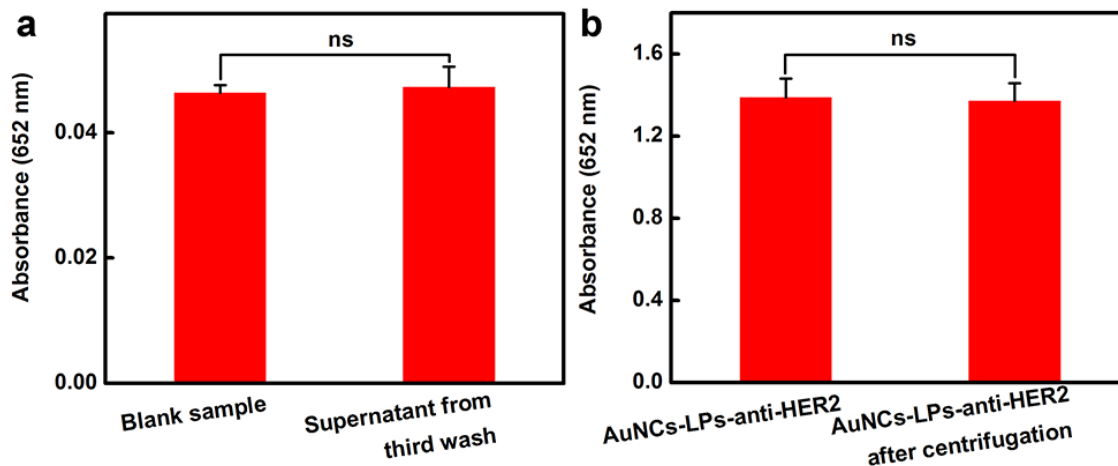


Figure S10. (a) Comparison of the peroxidase-like activity of free BSA-AuNCs-LPs-anti-HER2 incubated with the HER2-positive breast cancer cells in supernatant from the third wash and the blank sample. (b) Comparison of the enzyme activity of BSA-AuNCs-LPs-anti-HER2 with or without centrifugation (1000 rpm, 5 min) in the absence of cells. Error bars represent standard deviation of three independent measurements; ns=no significant difference ($P > 0.05$).

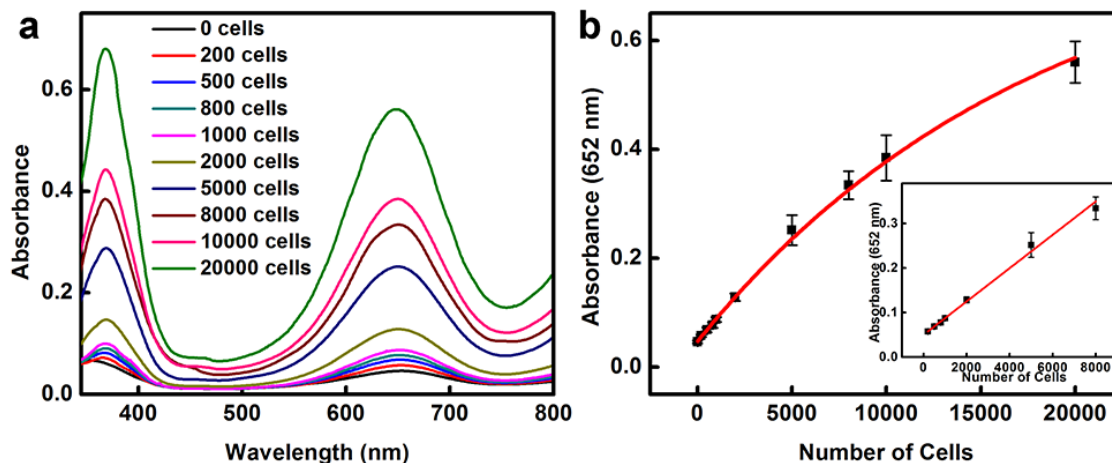


Figure S11. HER2-positive breast cancer cell detection by using BSA-AuNCs-anti-HER2. (a) The absorbance spectra changes upon analyzing different number of SKBR3 cells. (b) The absorption values at 652 nm depend on the number of SKBR3 cells. Inset: the linear plot. The error bars represent the standard deviation of three measurements. The detection limit is 200 cells.

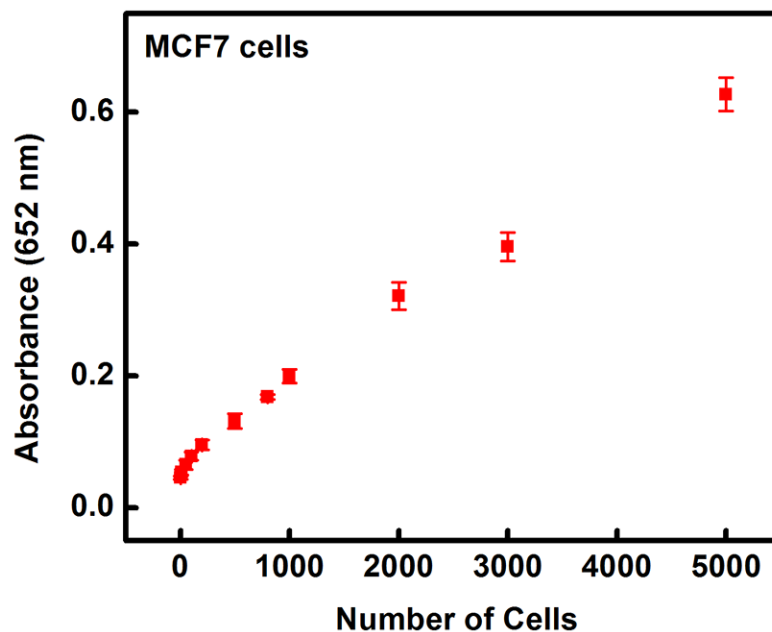


Figure S12. MCF7 cell detection by using BSA-AuNCs-LPs-anti-HER2. The absorption values at 652 nm depend on the number of MCF7 cells. The error bars represent the standard deviation of three measurements.

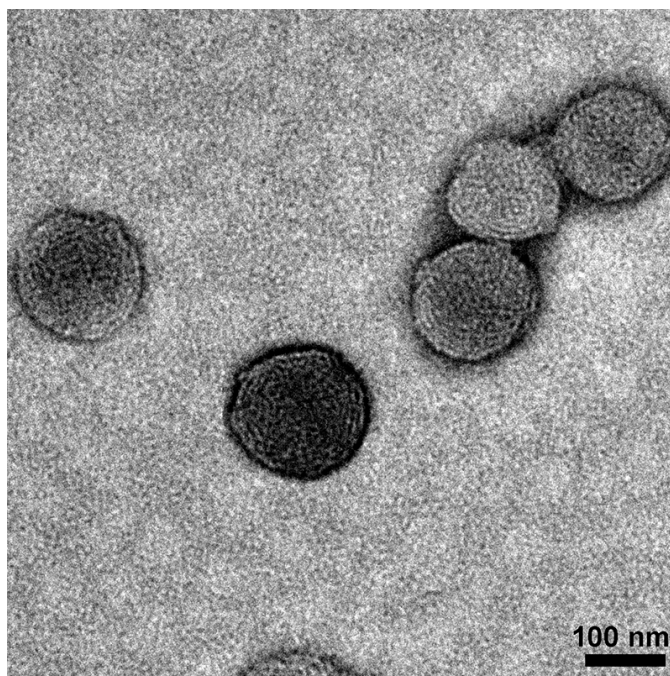


Figure S13. The TEM image of the BSA-AuNCs-LPs-AptMUC1.

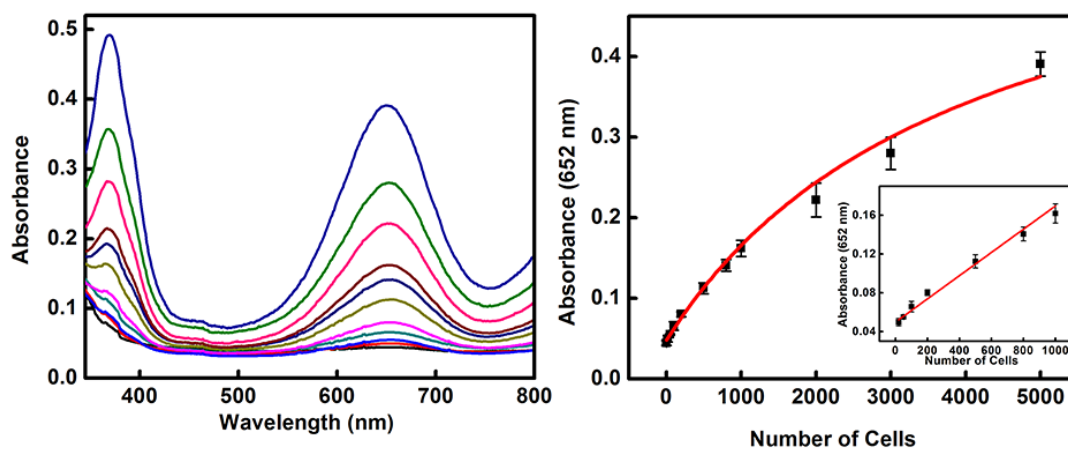


Figure S14. MCF7 cell detection by using BSA-AuNCs-LPs-AptMUC1. (a) The absorbance spectra changes upon analyzing different number of MCF7 cells. (b) The absorption values at 652 nm depend on the number of MCF7 cells. Inset: the linear plot. The error bars represent the standard deviation of three measurements.

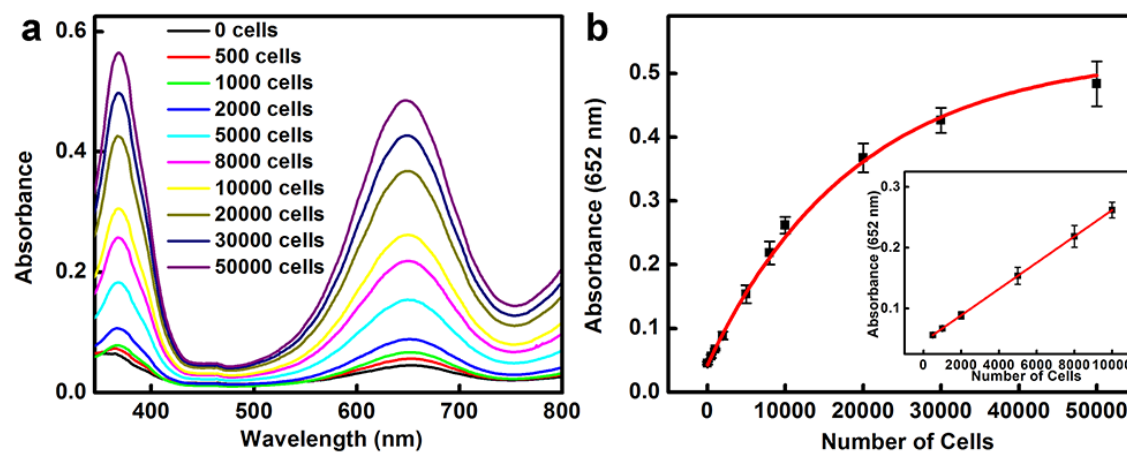


Figure S15. MCF7 cell detection by using AuNCs-AptMUC1. (a) The absorbance spectra changes upon analyzing different number of MCF7 cells. (b) The absorption values at 652 nm depend on the number of MCF7 cells. Inset: the linear plot. The error bars represent the standard deviation of three measurements. The detection limit is 500 cells.